Master of Science

Comparative study of autologous stromal vascular fraction and adipose-derived stem cells for recovery of renal function in a rat model of renal ischemia-reperfusion injury

The Graduate School

of the University of Ulsan

Department of Medical Science

Joomin Aum

Comparative study of autologous stromal vascular fraction and adipose-derived stem cells for recovery of renal function in a rat model of renal ischemia-reperfusion injury

Supervisor: Dalsan You

A Dissertation

Submitted to

the Graduate School of the University of Ulsan

In Partial Fulfillment of the Requirements

for the Degree of

Master of Science

by

Joomin Aum

Department of Medical Science

Ulsan, Korea

August 2020

Comparative study of autologous stromal vascular fraction and adipose-derived stem cells for recovery of renal function in a rat model of renal ischemia-reperfusion injury

This certifies that the dissertation

of Joomin Aum is approved.

Choung-Soo Kim ·

Committee Chair M.D., Ph D.

Nayoung Suh ·

Committee Member Ph D.

Dalsan You ·

Committee Member M.D., Ph D.

Department of Medical Science

Ulsan, Korea

August 2020

감사의 글

논문이 완성되기까지 도움 주신 많은 분들께 감사의 인사를 전합니다. 바쁘신 와중에도 소중한 시간을 내어 연구에 대한 조언해주신 김청수 교수님, 서나영 교수님 그리고 언제나 세심한 지도와 따뜻한 격려로 이끌어 주신 유달산 교수님께 진심으로 감사드립니다. 연구에 많은 도움과 힘이 되어 주신 장명진 선생님, 김유선 선생님, 김보현 선생님 모두 감사합니다.

ABSTRACT

Background: There is little study to compare the use of different cell types derived from adipose tissue or the optimal route for efficient and safe cell delivery in renal ischemia-reperfusion injury (IRI). The abilities of autologous stromal vascular fraction (SVF) and adipose-derived stem cells (ADSC), injected via three different routes, to protect renal function in a rat model of renal IRI were compared.

Materials and Methods: Ninety male Sprague-Dawley rats were randomly divided into 9 groups: sham, nephrectomy control, IRI control, renal arterial SVF injection, renal parenchymal SVF injection, tail venous SVF injection, renal arterial ADSC injection, renal parenchymal ADSC injection, and tail venous ADSC injection groups. The renal function was evaluated 4 days before and 1, 2, 3, 4, 7 and 14 days after surgical procedures to induce renal IRI. The histomorphometric studies were performed 14 days after surgical procedures.

Results: Renal parenchymal injection of SVF significantly reduced the extent of elevation in serum blood urea nitrogen and creatinine, compared with those for the IRI control group. Renal parenchymal injection of SVF significantly reduced the extent of decrease in glomerular filtration rate, compared with that for the IRI control group. In addition, collagen content was lower in the renal parenchymal SVF injection group than in the IRI control group. Apoptosis was decreased in the renal parenchymal SVF injection group, compared with that in the IRI control group, and proliferation was increased. The expressions of anti-

oxidative makers such as glutathione reductase and glutathione peroxidase were higher in the renal parenchymal SVF injection group than in IRI control group.

Conclusions: Our study suggests that renal function is effectively rescued from renal IRI through renal parenchymal injection of SVF by enhanced anti-fibrotic, anti-apoptotic and anti-oxidative effects.

CONTENTS

LIST OF FIGURES

INTRODUCTION

Acute kidney injury (AKI) is characterized by a deterioration in renal function over a period of hours to days, causing the kidney to fail to excrete nitrogenous waste products and maintain fluid and electrolyte homeostasis [1)]. Ischemia-reperfusion injury (IRI) is a common etiology of AKI in hospitals [1, 2)]. IRI is the aggravation of tissue damage upon reestablishment of circulation after ischemia. Renal IRI is an inevitable consequence of kidney transplantation from deceased donors, on-pump cardiac surgery and nephron-sparing surgery. Unfortunately, current treatment to reduce the extent of renal IRI is primarily supportive.

Recently, cell-based therapies have been attempted with some promising results in AKI [3-8)]. Both cultured and uncultured cells have been demonstrated to improve tissue regeneration and functional recovery in AKI [9-13)]. We also found that renal arterial injection of hypoxic preconditioned mesenchymal stem cells (MSC) or adipose tissue-derived stromal vascular fraction (SVF) rescues renal function in a rat model of renal IRI [14, 15)]. In spite of several preclinical studies promising the efficiency of cell-based therapy in kidney diseases, its clinical trials remained in primitive steps, and are associated with some problems such as cell sources and delivery [16)].

There are several concerns regarding the implantation of cultured stem cells into humans, including the risks of xenogenic nutritional sources, microbial contamination, and tumorigenesis [17)]. To avoid these risks, uncultured/heterogeneous SVF has been proposed as an easier and safer way to use stem and progenitor cells derived from adipose tissue. Recent preclinical and clinical trials have focused on the use of SVF in treating various kidney diseases [18-21)]. However, there is little study to compare the use of different cell types derived from adipose tissue in renal IRI [22)]. In addition, the optimal route for efficient and safe cell delivery is little known [14)]. Therefore, we compared the effects of autologous SVF and

adipose-derived stem cells (ADSC), injected via three different routes, on renal function in a rat model of renal IRI.

MATERIALS AND METHODS

Animal Care and Study Design

All aspects of animal care and treatment and the surgical procedures used conformed to the eighth edition of the Guide for the Care and Use of Laboratory Animals, published in 2011. The protocols for performing animal experiments were approved by the Institutional Animal Care and Use Committee of Asan Medical Center (2016–12–068). Ninety 11-week-old male Sprague-Dawley rats were purchased from Orient Bio Inc. (Gyeonggi, Korea, http://www.orient.co.kr) and housed for 1 week for acclimatization. During experiments, rats were maintained under a 12-hour: 12-hour light/dark cycle (lights on at 8 a.m. and off at 8 p.m.), at a temperature of 22°C ± 2°C, and at a humidity level of 50%–55%, with ad libitum access to food and water.

At 12 weeks old, the rats were randomly divided into 9 groups (10 animals per group): sham, nephrectomy control, IRI control, renal arterial SVF injection, renal parenchymal SVF injection, tail venous SVF injection, renal arterial ADSC injection, renal parenchymal ADSC injection, and tail venous ADSC injection groups. Rats in the ADSC group underwent bilateral paratesticular fat excision via scrotal incision to isolate and culture ADSC. At 14 weeks old, rats in the SVF group underwent bilateral paratesticular fat excision via scrotal incision to isolate SVF. At the same time, surgical procedures were performed to induce renal IRI. SVF and ADSC were injected into different three routes in the SVF and ADSC groups, respectively. The renal function of all the rats was evaluated 4 days before and 1, 2, 3, 4, 7 and 14 days after surgical procedures. They were sacrificed 14 days after surgical procedures, and the kidney tissues were then collected for histological examination. The study design is outlined in Figure 1.

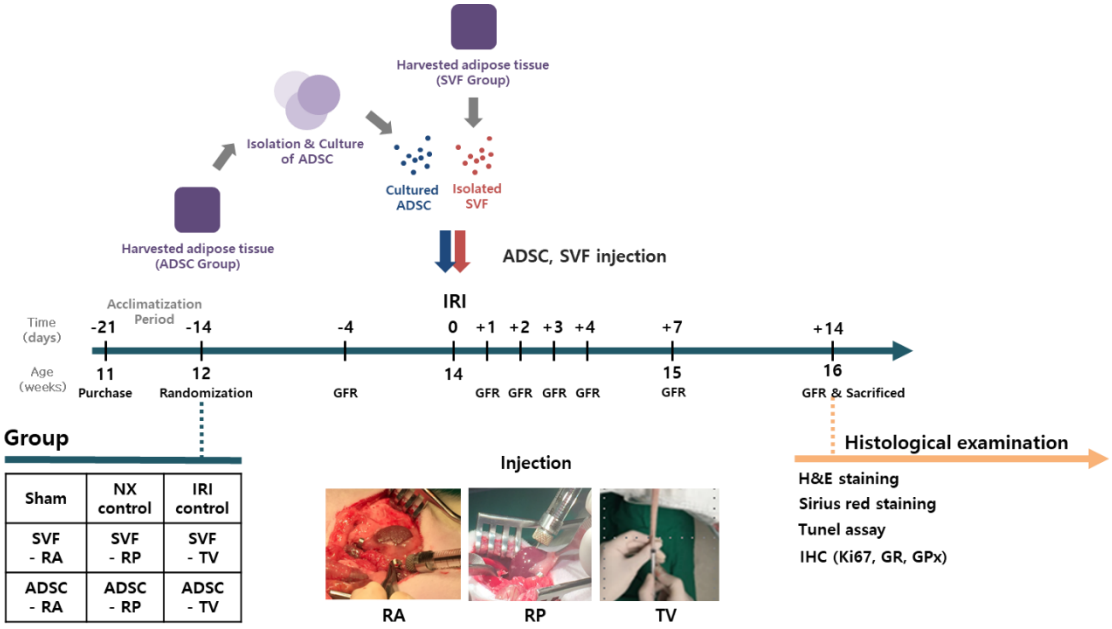

Figure 1. Study design. Abbreviations: ADSC, adipose-derived stem cell; GFR, glomerular filtration rate; GR, glutathione reductase; GPx, glutathione peroxidase stain; H&E, hematoxylin and eosin stain; IHC, immunohistochemistry; IRI, ischemia-reperfusion injury; NX, nephrectomy; RA, renal arterial; RP, renal parenchymal; SVF, stromal vascular fraction; TV, tail venous.

Isolation of SVF and Culture of ADSC

Adipose tissue was harvested from paratesticular fats via scrotal incision at randomization (ADSC group) or shortly before surgical procedures to induce renal IRI (SVF group). ADSC were cultured according to a standardized protocol [23, 24]. Adipose tissue was enzymatically digested for 30 min at 37°C in 0.075% collagenase type I (Thermo Fisher Scientific Inc., Waltham, MA, http://www.thermofisher.com). The cell suspension was passed through a 100-mm pore-sized filter to remove undissociated tissue, neutralized by addition of Dulbecco's modified Eagle's medium (DMEM) containing 10%fetal bovine serum (FBS), and centrifuged at 800g for 5 min. The stromal cell pellet was resuspended in DMEM containing 10% FBS and 1% antibiotic-antimycotic solution. Cultures were maintained at subconfluent levels (80%) at 37℃ in 5% CO_2. Cells were passaged using trypsin/EDTA (Thermo Fisher Scientific Inc.) as required. The resuspended cells were plated at a density of 2×10^3 cells per cm^2 and cultured until passage 3 before being injected.

To determine whether the processed lipoaspirate cells were characteristic of SVF or ADSC, flow cytometry were performed with a FACScan argon laser cytometer (BD Biosciences, San Jose, CA, http://www.bdbiosciences.com) according to a previous study [25]. Briefly, cells were harvested in 0.25% trypsin/EDTA and fixed for 30 min in ice-cold 2% formaldehyde. The fixed SVF was washed in flow cytometry buffer (2% bovine serum albumin, 0.1% sodium azide in PBS) and incubated for 30 min in flow cytometry buffer containing anti-CD45PE-Cy7, CD11b/cPE, CD31PE, CD73FITC, and CD90FITC (BD Biosciences). The fixed ADSC were washed in flow cytometry buffer and incubated for 30 min in flow cytometry buffer containing anti-CD29FITC, CD34FITC, CD44FITC, CD45FITC (BD Biosciences).

Differentiation of ADSC

Differentiation of ADSC was confirmed as described previously [26].The ADSC at the fourth passage were incubated with a StemPro Adipogenesis Differentiation Kit and StemPro Osteogenesis Differentiation Kit for 14 days and a StemPro Chondrogenesis Differentiation kit (Thermo Fisher Scientific Inc.) for 21 days, and the medium was changed every 3–4 days. The adipogenic differentiation was confirmed using Oil Red O (Sigma-Aldrich, St. Louis, MO, http://www.sigmaaldrich.com), the osteogenic differentiation was confirmed using 2% alizarin red S (ScienCell, Carlsbad, CA, https://sciencellonline.com), and the chondrogenic differentiation was confirmed using Alcian blue. The cells were photographed with an inverted microscope (Olympus, Tokyo, Japan, http://www.olympus-global.com).

Labeling and Tracking

SVF and ADSC were labeled with the fluorescent dye PKH-26 (Sigma-Aldrich). The cells suspension was mixed with a solution of PKH-26 dye at concentrations of 1×10^6 cells per ml and incubated at 25°C for 5 min. An equal volume of serum was added to stop the staining reaction. The sample was diluted with an equal volume of the Diluent C and centrifuged. The cells were resuspended in saline buffer and injected into each route. Cross-sections of kidney injected with PKH-26-labeled SVF and ADSC were observed using the fluorescent microscope.

IRI and Cell Transplantation

Each rat was intramuscularly anesthetized with 0.3 ml of tiletamine (Zoletil; Virbac Laboratories, Carros, France, https://corporate.virbac.com) and xylazine hydrochloride (Rompun; Bayer, Leverkusen, Germany, https://www.bayer.com) in a 4:1 mixture. Laparotomy was performed in the sham group and right nephrectomy was performed in the nephrectomy control group, while right nephrectomy was performed and IRI of the left

kidney was induced in the other seven groups. IRI induction was performed in the left kidney as described previously [15]. In the renal arterial injection groups, 100 µl amount of a cell suspension in PBS (1×10^6 cells) was injected into the aorta after clamping the aorta above and below the left renal artery using bulldog clamp (Fine Science Tools, Heidelberg, Germany, https://www.finescience.com), immediately prior to the induction of renal IRI. And then the left renal artery was clamped with a bulldog clamp for 40 min. The 33-gauge Hamilton syringe (Hamilton Company, Zurich, Switzerland, https://www.hamiltoncompany.com) was used to minimize the damage of aorta. The injection site was closed using TachoSil® Sealant matrix (Takeda Austria GmbH, Linz, Austria, https://www.takeda.com), and the clamps were removed to restore aortic blood flow after 10 min. In the renal parenchymal injection groups, the Hamilton syringe needle containing same amount of a cell suspension was pierced from the lower pole to the upper pole of the kidney. While pulling out the needle, the cells were gradually released from the syringe. In the tail venous injection groups, same amount of a cell suspension was injected via the tail vein using a 26-gauge Kovax-syringe (Koreavaccine, Gyeonggi, Republic of Korea, http://www.koreavaccine.com).

Observations of Clinical Signs and Measurements of Body Weight and Food Consumption

All the rats were observed daily for general condition, motility, excreta, and other factors. The presence of moribund conditions or mortality was also recorded. The body weight was measured 4 days before and 1, 2, 3, 4, 7 and 14 days after surgical procedures. The food consumption was measured weekly prior to surgical procedures and during the observational period. The amount of food consumed was estimated by subtracting the amounts of leftover food from the amounts of presented food.

Determination of Renal Function

Serum blood urea nitrogen (BUN), serum and urine creatinine levels were measured 4 days before and 1, 2, 3, 4, 7 and 14 days after surgical procedures. Urine was collected from animals in a metabolic cage for 24 hours, to estimate 24 h urine volume. The glomerular filtration rate (GFR) was assessed by creatinine clearance rate (CCr) based on serum and urine creatinine levels and computed with the following formula: CCr (mL/min/100 g) = (urine creatinine × 24 h urine volume × 100) / (serum creatinine × 1440 × body weight). Quantification of BUN and creatinine levels were performed using standard laboratory equipment at our hospital.

Kidney Harvest

The left kidney of all groups was harvested for histological examination. The weight of the left kidneys was measured after harvest. The kidney was cut in half and the cross-section was visually observed. Half of each kidney was cryopreserved in liquid nitrogen for protein extraction or immunofluorescence staining. The remaining half was fixed in 4% paraformaldehyde and embedded in paraffin prior to sectioning and immunohistochemistry analysis.

Hematoxylin and Eosin Staining and Histopathological Scoring

Kidney tissues were sectioned at 4 μm intervals and hematoxylin & eosin (H&E) stain was performed for optic microscopic analysis. After drying for 1 hour at 60℃ oven, tissue sections were deparaffinized in xylene I, II and xylene III for 10 min each. After rehydrating through graded ethanol (100%, followed by 90% to 70%; 1 min each), sections were washed 3 times with distilled water. The sections were stained with Harris Hematoxylin solution (Sigma-Aldrich, St. Louis, MO) for 5 min and washed three times in distilled water, and then washed again in 0.5% acid alcohol solution for 3 times followed by 3 times of washing in

distilled water. After stained with Eosin Y solution (Sigma-Aldrich, St. Louis, MO) for 10 s, the sections were rinsed with distilled water for 3 times. The slides were rehydrated in ethanol solutions of decreasing dilutions (70%, followed by 80%, and so on) respectively (If there was insufficient staining, reverse staining was done. If eosin stain was dense, sections were decolorized in absolute ethanol for 5 to 10 min). Repeatedly the sections were washed in xylene I, II and xylene III finally for 10 min. After then, sections were covered with the coverslip using Permount™ mounting medium. Histopathological scoring was estimated on the basis of previous studies in a blinded fashion [27]. Histopathological scoring was quantitated by calculation of the degree of cast formation, interstitial inflammation, tubular dilatation, glomerulus degeneration in 10 randomly chosen, non-overlapping fields.

Sirius Red Staining

After drying for 1 hour in 60℃ oven, the slides were dipped in Xylene I and Xylene II, treated with Xylene III, and dipped in ethanol solutions in the following order: 100% to 90% and 80% to 70%, 1 min each and washed in distilled water for 3 times. After dipping slides in distilled water thrice, we dipped them in the Harris hematoxylin solution (Sigma-Aldrich, St. Louis, MO) for 5 min. Then the slides were rinsed three times in distilled water, the area around the tissue was marked with a PAP pen. Pico Sirius Red reagent 60 µl was dropped on the slides and incubated for 20 min. After dipping twice in the acid solution, the slides were washed three times using distilled water, then rehydrated through graded ethanol (70%, 80%, 90%, and 100%). Repeatedly, sections were cleared by incubation in xylene I, II, III for 10 min each and mounted using permanent mounting media.

TUNEL Assay

Terminal deoxynucleotidyl transferase (TdT) -mediated dUTP nick end labeling (TUNEL) for the detection of apoptotic cells was performed using in situ cell death detection kit

according to manufacturer's protocol (Roche Molecular Biochemicals, Mannheim, Germany, https://life science.roche.com/shop/home). TUNEL assay confirmed the degree of apoptosis in tissue due to IRI to clarify the effect of MSC. Under light microscopy, TUNEL-stained sections were observed with the positive-stained cell count.

Unstained slides were placed in a 60℃ dryer and dissolved in paraffin for 1 hour to allow the tissue to adhere well. Each sectioned specimen was deparaffinized in xylene I, II and III for 10 min each and rehydrated in ethanol solutions of increasing dilutions (100%, followed by 90%, and so on to 70%) for 1 min each. the sections were washed in distilled water for 3 min in the same manner. For antigen retrieval, the slides were placed into a pretreatment solution (heat-induced epitope retrieval solution/ target retrieval solution). Through incubation for 5 min in a microwave oven followed by cooling down another 10 min, sections were washed in wash buffer (0.1% Tween-20 in PBS) for 5 min. After washing, the protein blocking serum-free ready-to-use (Dako, Glostrup, Denmark, http://www.dako.com) reagent containing 20% FBS was dropped into the sections and they were incubated in a humid chamber for 30 min in a humid chamber. Then the sections were washed in PBS for 5 min, gently wiped after removed from the buffer and shaken well. Subsequently, 50 μl of the tunnel reaction mixture was dispensed onto the slides and incubated in a 37℃ humid chamber for 1 hour. Then the slides were rinsed in PBS for 5 min. And then, 50 μl of Converter-POD (Converter-Peroxidase) were dispensed and incubated in a 37℃ humid chamber for 30 min. The slides were covered with parafilm (Bemis company inc., Oshkosh, WI, http://www.bemis.com) and spread evenly followed by washing with fresh PBS for 3 times. The sections were washed in the buffer and shaken well. Then, 50 μl of DAB-starting working solution (substrate buffer 1 mL + DAB chromogen 20 μl) was added to the specimens and incubated for 10 min until appropriate color appeared. Then the slides were washed 3 times in fresh PBS again. The slides were counterstained with hematoxylin for 5s. Afterwards, the slides were washed 3 times in fresh PBS and rehydrated in ethanol solutions

of decreasing dilutions (70%, followed by 80%, 90%, 100%) for 1 min each. Then the sections were cleared in xylene I, II respectively and then placed in new xylene for 10 min and mounted using prepared coverslip.

Immunohistochemistry

Kidney sections (4 μm thick) were prepared for immunohistochemistry analysis from rats of each group. Tissue sections were placed on microslides and deparaffinized in xylene, hydrated in increasingly diluted serial ethanol solutions, and immersed in 3% H_2O_2 to quench endogenous peroxidase activity. To permit antigen retrieval, all sections were microwaved for 15 min in Tris-EDTA buffer (pH 9.0), prepared in distilled water. Next, the sections were incubated for 2 hours at an ambient temperature with anti-Ki67 (1:200, Abcam, Cambridge, MA, http://www.abcam.com), anti-glutathione reductase (GR; 1:2000, Abcam), and anti-glutathione peroxidase (GPx; 1:2000, Abcam) antibodies. After washing, the slides were incubated using a biotin-free polymeric horseradish peroxidase–linker antibody conjugate system (Dako) for 30 min at an ambient temperature. The slides were washed, and chromogen development was performed for 10 min. The slides were counterstained with Meyer's hematoxylin and mounted using Immu-mount (Thermo Fisher Scientific Inc.). For image analysis, four randomly selected kidney fields per animal in both the cortex and the medulla (40 kidney fields per group) were photographed. Images were recorded at 40× magnification via a Panoramic viewer program software (3DHistech, Budapest, Hungary, https://www.3dhistech.com). All images were analyzed by using Adobe Photoshop CS2 (Adobe, San Jose, CA, https://www.adobe.com) to quantify signals. The results of proliferation are presented as the percentage of Ki67-positive areas to the total area in each field (cortex and medulla). A semiquantitative analysis was used to express GR and GPx as the percentage of the positive area in a blind fashion.

Statistical Analysis

Categorical variables were expressed as frequency and percent, and continuous variables as mean ± standard error (SE). We used one-way analysis of variance (ANOVA) followed by Turkey's honest significant difference test for post hoc comparisons of multiple group analysis. Statistical significance was defined as $P < 0.05$, $P < 0.01$ or $P < 0.001$; $P \geq 0.05$ was not considered significant. All statistical analysis was performed using SPSS Statistics, version 21 (IBM Corporation, Armonk, NY, http://www-01ibm.com).

RESULTS

Characterization of SVF and ADSC

To characterize SVF and ADSC, CD marker profiles characteristic of SVF and ADSC were examined using flow cytometry. Flow cytometric analysis showed that SVF was made up of over half CD45+ cells (blood-derived cells), 1.5% CD45-/CD31+ (endothelial cells) and 42% CD45-/CD31- cells. CD73 and CD90 were expressed by almost half of CD45- cells (stromal cells). Flow cytometric analysis showed that of cultured ADSC, 99.9% expressed CD29, 1.4% expressed CD34, 99.1% expressed CD44, 0.1% expressed CD45. The multilineage differentiation capacity was confirmed by observation of adipogenic, osteogenic, and chondrogenic differentiations after 3 weeks of culture in appropriate induction media (Figure 2).

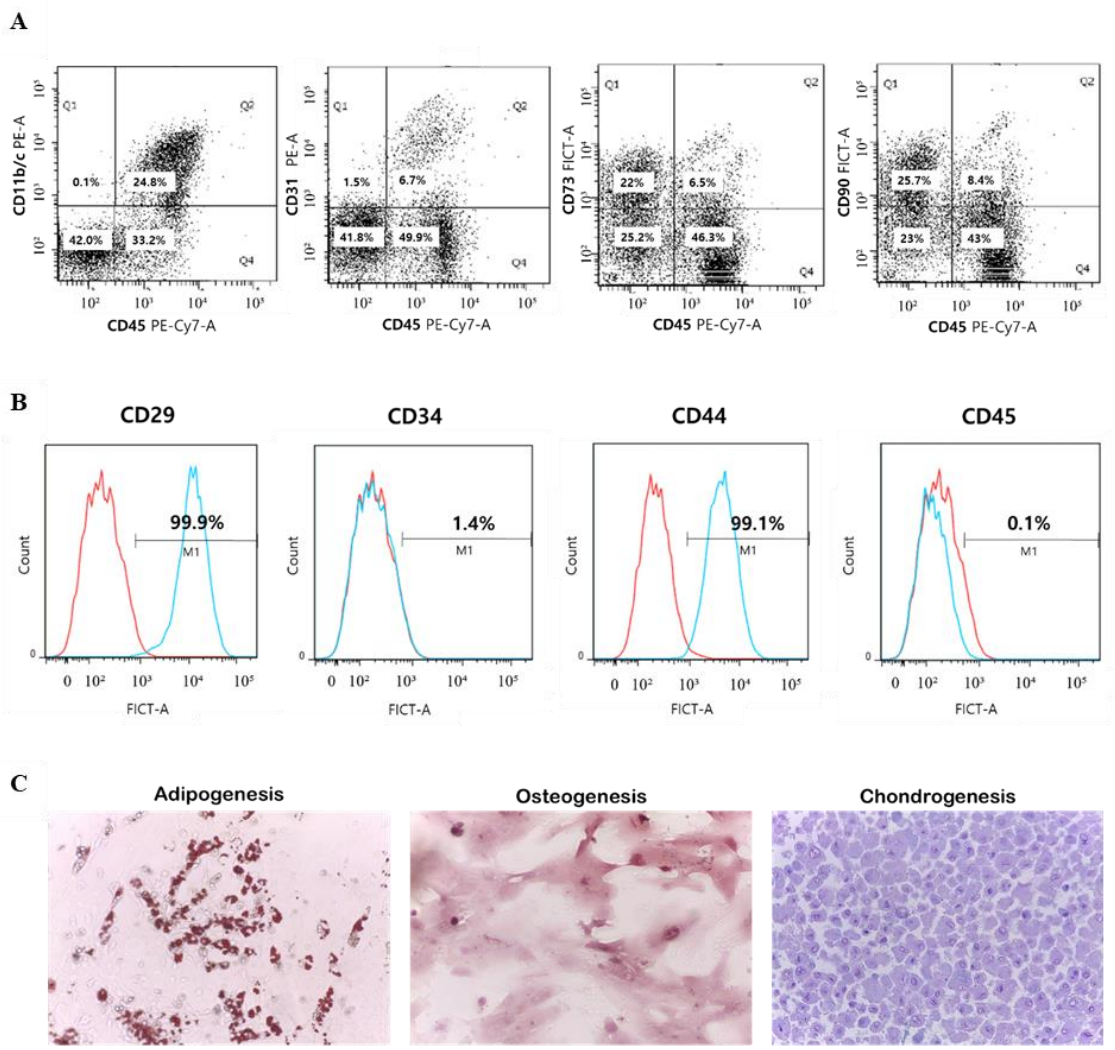

Figure 2. (A) Representative flow cytometry histograms of SVF. (B) Representative flow cytometry histograms of ADSC. (C) Appearance of ADSC after 3 weeks of induction of adipogenic, osteogenic, and chondrogenic differentiation. Magnification, X100 in adipogenesis and osteogenesis and X400 in chondrogenesis. Abbreviations: FITC, fluorescein isothiocyanate; PE, phycoerythrin.

Clinical Signs and Body Weight and Food Consumption

Two cases of mortality in each group were observed in the renal arterial injection of SVF and renal arterial injection of ADSC, respectively (Figure 3A). There were no significant differences in body weight and food consumption among the groups (Figure 3B and C).

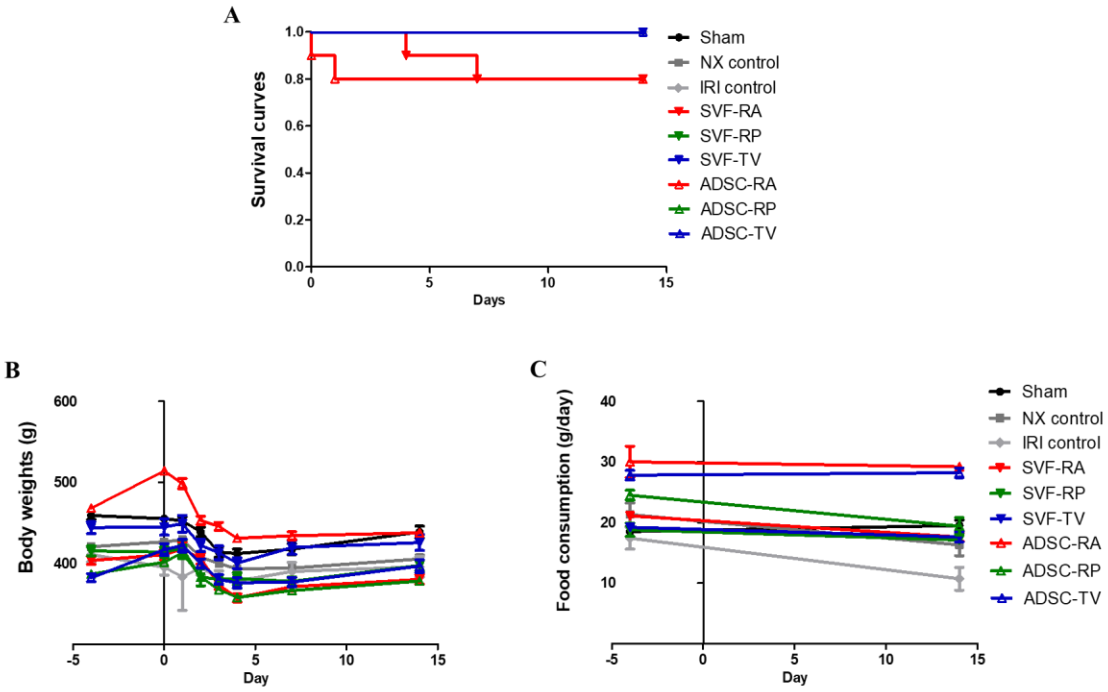

Figure 3. (A) Survival curves. (B) Changes in body weight and (C) Food consumption of each group during the experiment.

Abbreviations: ADSC, adipose-derived stem cell; IRI, ischemia-reperfusion injury; NX, nephrectomy; RA, renal arterial; RP, renal parenchymal; SVF, stromal vascular fraction; TV, tail venous.

Effects of SVF and ADSC on Renal Function

Renal parenchymal injection of SVF significantly reduced the extent of elevation in serum BUN, compared with that in the IRI control group, at 1 day after IRI ($P<0.001$) (Figure 4A). Renal parenchymal injection of SVF significantly reduced the extent of elevation in serum creatinine, compared with that in the IRI control group, at 1 and 7 days after IRI ($P<0.001$ and <0.05) (Figure 4B). Renal parenchymal injection of SVF significantly reduced the extent of decrease in GFR, compared with that in the IRI control group, at 1, 2 and 14 days after IRI ($P<0.001$, <0.001 and <0.01). In addition, tail venous injection of SVF significantly reduced the extent of decrease in GFR, compared with that in the IRI control group, at 4 days after IRI ($P<0.01$) (Figure 4C).

The weight of the left kidney was significantly increased in all the treated groups except renal parenchymal SVF injection, compared with that in the sham group (Figure 4D). No gross differences in kidney cross-sections were observed (Figure 4E).

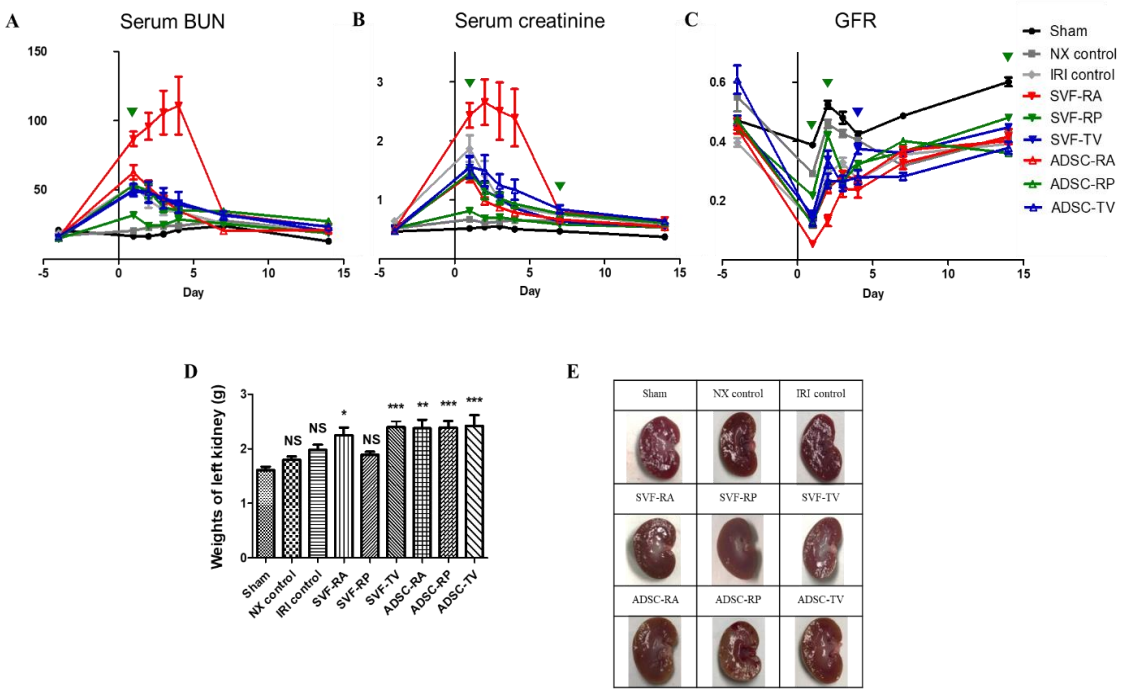

Figure 4. (A) Changes in serum BUN, (B) serum creatinine and (C) GFR of each group during the experiment. Green and blue-colored inverted triangles indicate statistically significant difference in the SVF-RP and SVF-TV groups compared with the IRI control group, respectively. (D) Weights of left kidney after harvest. NS, $P > 0.05$; *, $P < 0.05$; **, $P < 0.01$; ***, $P < 0.001$ compared with the sham group. (E) Representative pictures of cross-sectioned left kidney.

Abbreviations: ADSC, adipose-derived stem cell; IRI, ischemia-reperfusion injury; NX, nephrectomy; RA, renal arterial; RP, renal parenchymal; SVF, stromal vascular fraction; TV, tail venous.

Histopathological Scoring and Fibrosis of Kidney Tissue

Histopathological score was significantly higher in the IRI control group than in the sham and nephrectomy control groups. There were no significant differences in histopathological score among the IRI control and all the treated groups (Figure 5).

Sirius red staining revealed that collagen content was significantly higher in the IRI control group than in the sham and nephrectomy control groups in both the cortex and medulla. Collagen content was significantly lower in the renal parenchymal SVF injection group than in the IRI control group in both the cortex and medulla (Figure 6).

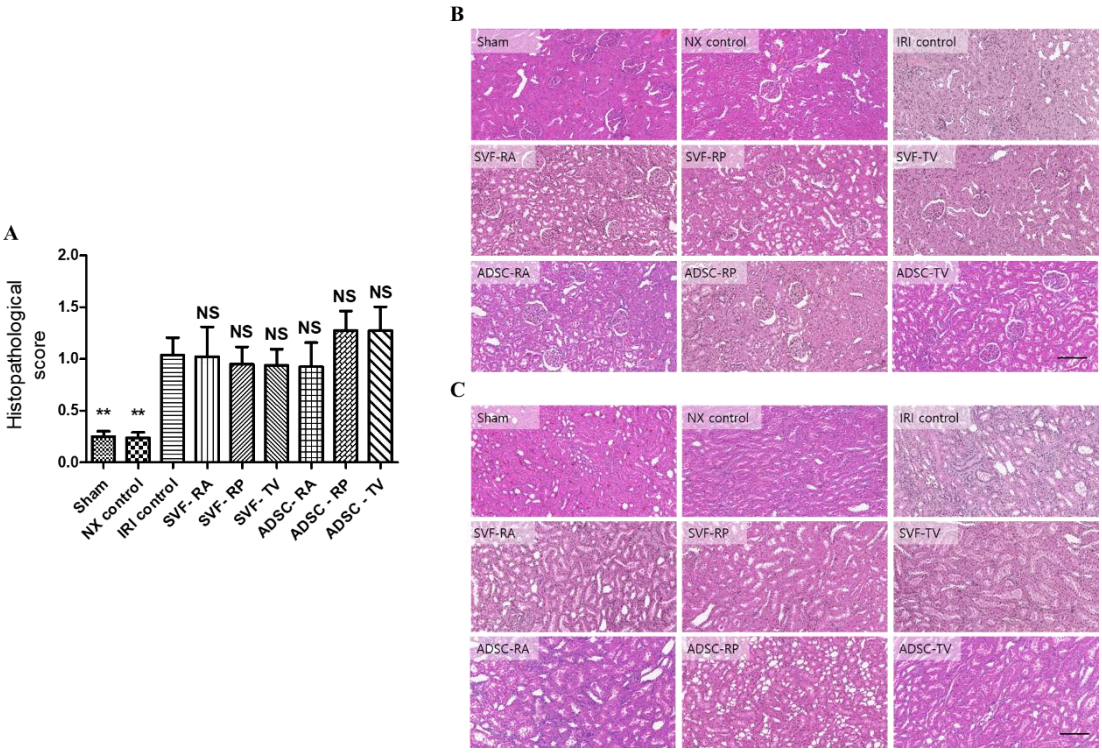

Figure 5. H&E stain for histopathological score determination. (A) Histopathological score in the random cortex and medulla area (B) representative photomicrographs of cortex (C) representative photomicrographs of medulla. Scale bar 50 μm. NS, $P > 0.05$; **, $P < 0.01$compared with the IRI control group. Nonparametric tests (Kruskal-Wallis and Mann-Whitney tests) were used for statistical analysis.

Abbreviations: ADSC, adipose-derived stem cell; IRI, ischemia-reperfusion injury; NX, nephrectomy; RA, renal arterial; RP, renal parenchymal; SVF, stromal vascular fraction; TV, tail venous.

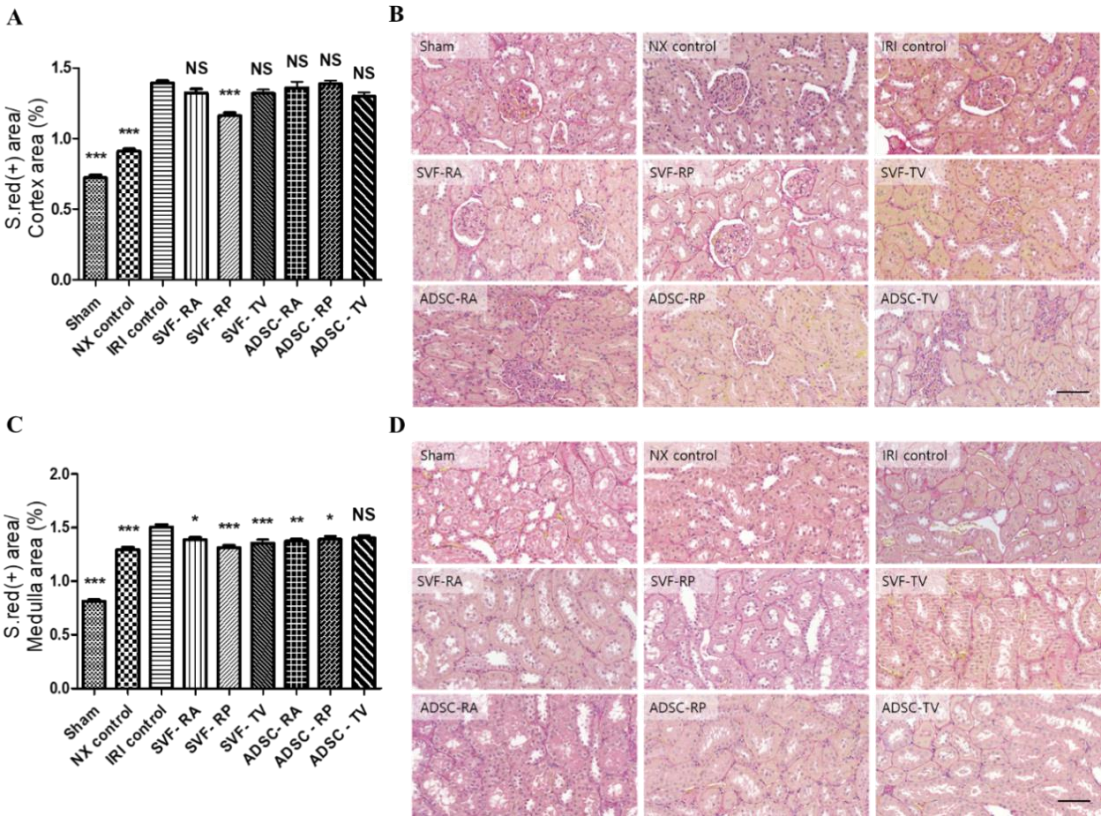

Figure 6. Sirius red staining for determining the degree of fibrosis. (A) Ratio of the area stained positive for Sirius red to the random cortex area and (B) representative photomicrographs. (C) Ratio of the area stained positive for Sirius red to the random medulla area and (D) representative photomicrographs. Scale bar 100 μm. NS, $P > 0.05$; *, $P < 0.05$; **, $P < 0.01$; ***, $P < 0.001$ compared with the IRI control group.

Abbreviations: ADSC, adipose-derived stem cell; IRI, ischemia-reperfusion injury; NX, nephrectomy; RA, renal arterial; RP, renal parenchymal; SVF, stromal vascular fraction; TV, tail venous.

Apoptosis and Proliferation Markers of Kidney Tissue

TUNEL assay revealed that apoptosis was significantly increased in the IRI control group, compared with that in the sham and nephrectomy control groups, in both the cortex and medulla. Apoptosis was significantly decreased in all the treated groups, compared with that in the IRI control group, in both the cortex and medulla (Figure 7).

Ki67 stain revealed that proliferation was significantly increased in the IRI control group, compared with that in the sham group, in both the cortex and medulla. Proliferation was significantly increased in all the treated groups, compared with that in the IRI control group, in the cortex and in the renal arterial and parenchymal SVF injection groups in the medulla, respectively (Figure 8).

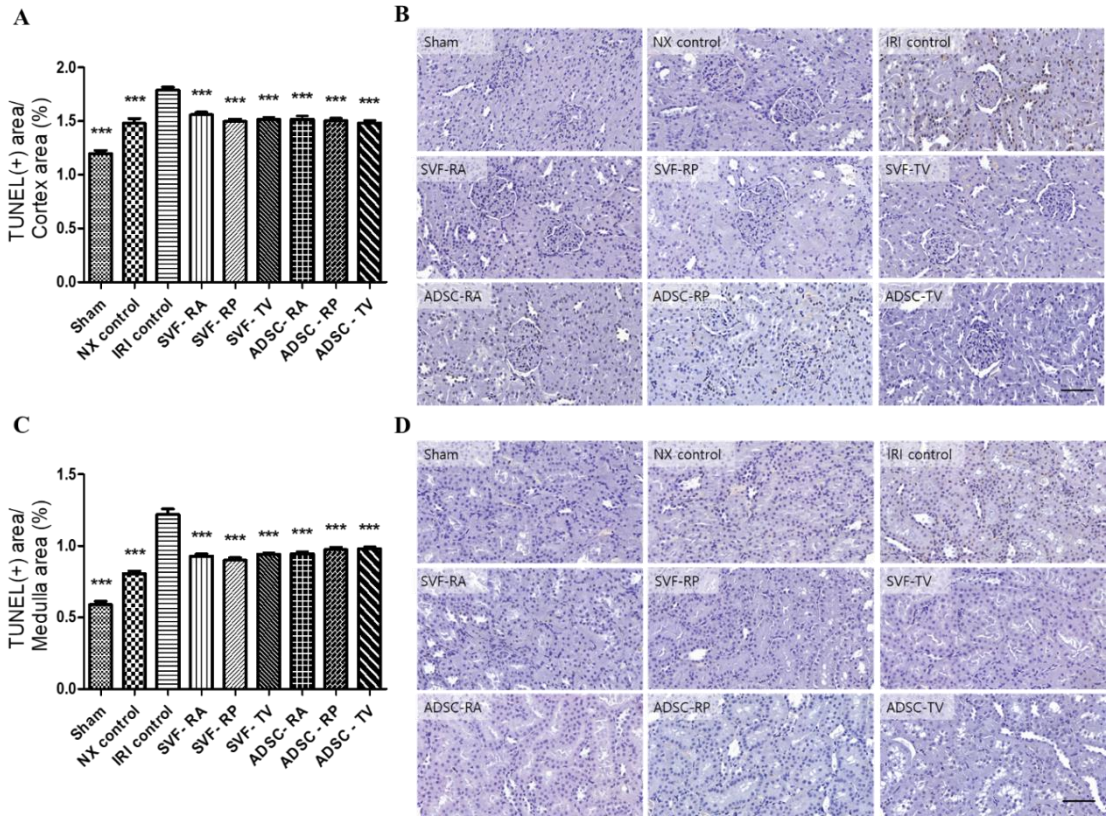

Figure 7. TUNEL assay for determining the degree of apoptosis. (A) Ratio of the area stained positive for TUNEL to the random cortex area and (B) representative photomicrographs. (C) Ratio of the area stained positive for TUNEL to the random medulla area and (D) representative photomicrographs. Scale bar 100 μm. ***, $P < 0.001$ compared with the IRI control group.

Abbreviations: ADSC, adipose-derived stem cell; IRI, ischemia-reperfusion injury; NX, nephrectomy; RA, renal arterial; RP, renal parenchymal; SVF, stromal vascular fraction; TV, tail venous.

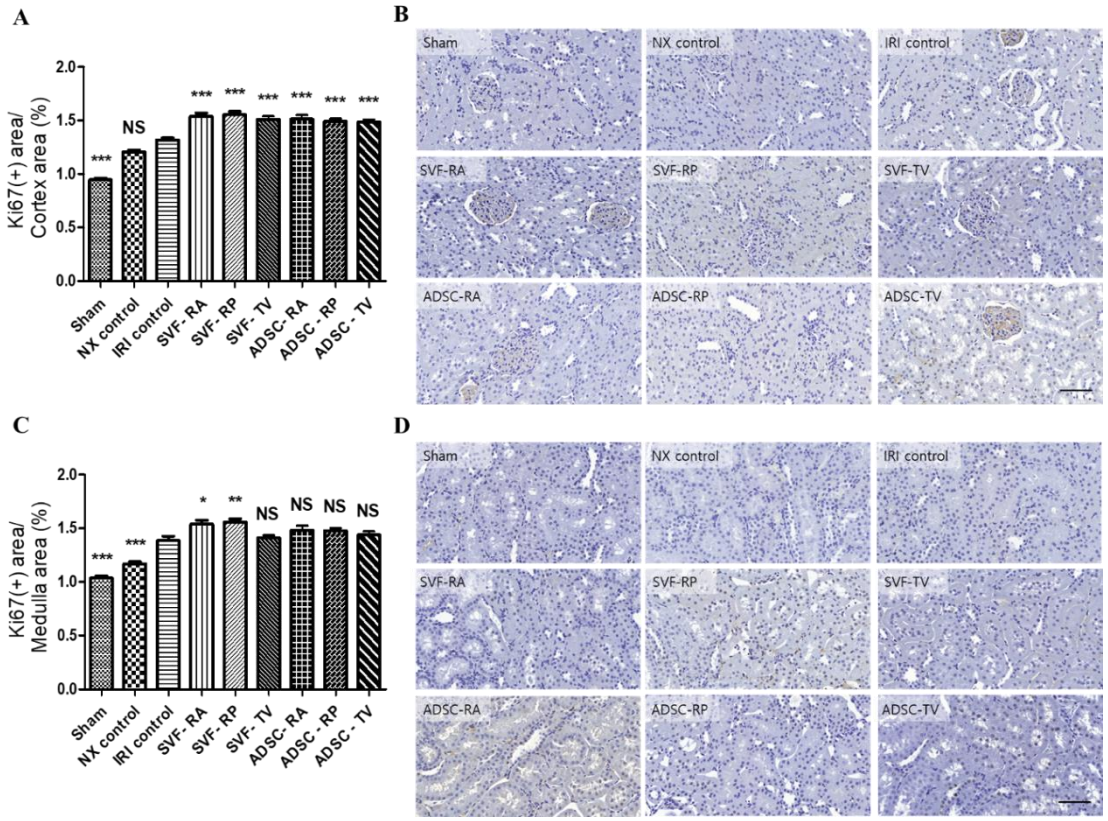

Figure 8. Ki67 stain for determining the degree of proliferation. (A) Ratio of the area stained positive for Ki67 to the random cortex area and (B) representative photomicrographs. (C) Ratio of the area stained positive for Ki67 to the random medulla area and (D) representative photomicrographs. Scale bar 100 μm. NS, $P > 0.05$; *, $P < 0.05$; **, $P < 0.01$; ***, $P < 0.001$ compared with the IRI control group.

Abbreviations: ADSC, adipose-derived stem cell; IRI, ischemia-reperfusion injury; NX, nephrectomy; RA, renal arterial; RP, renal parenchymal; SVF, stromal vascular fraction; TV, tail venous.

Anti-oxidative Markers of Kidney Tissue

The GR-positive percentage area was significantly higher in the IRI control group than in the sham group in both the cortex and medulla. It was significantly higher in all SVF treated and renal parenchymal ADSC injection groups than in the IRI control group in the cortex and in all treated groups in the medulla, respectively (Figure 9).

The GPx-positive percentage area was significantly higher in the IRI control group than in both the sham and nephrectomy control groups in both the cortex and medulla. It was significantly higher in all treated groups than in IRI control group in the cortex and in both the renal parenchymal SVF and tail venous ADSC injection groups in medulla, respectively (Figure 10).

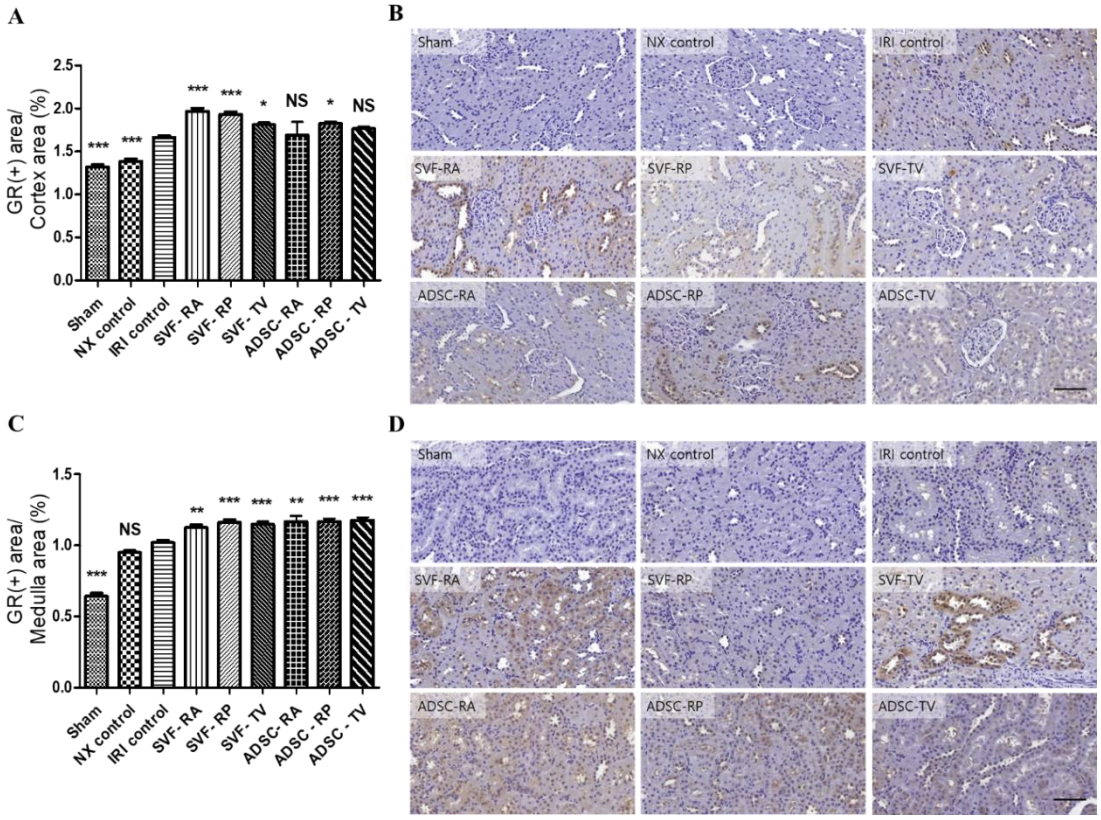

Figure 9. GR stain for determining the degree of Anti-oxidation. (A) Ratio of the area stained positive for GR to the random cortex area and (B) representative photomicrographs. (C) Ratio of the area stained positive for GR to the random medulla area and (D) representative photomicrographs. Scale bar 100 μm. NS, $P > 0.05$; *, $P < 0.05$; **, $P < 0.01$; ***, $P < 0.001$ compared with the IRI control group.

Abbreviations: ADSC, adipose-derived stem cell; IRI, ischemia-reperfusion injury; NX, nephrectomy; RA, renal arterial; RP, renal parenchymal; SVF, stromal vascular fraction; TV, tail venous.

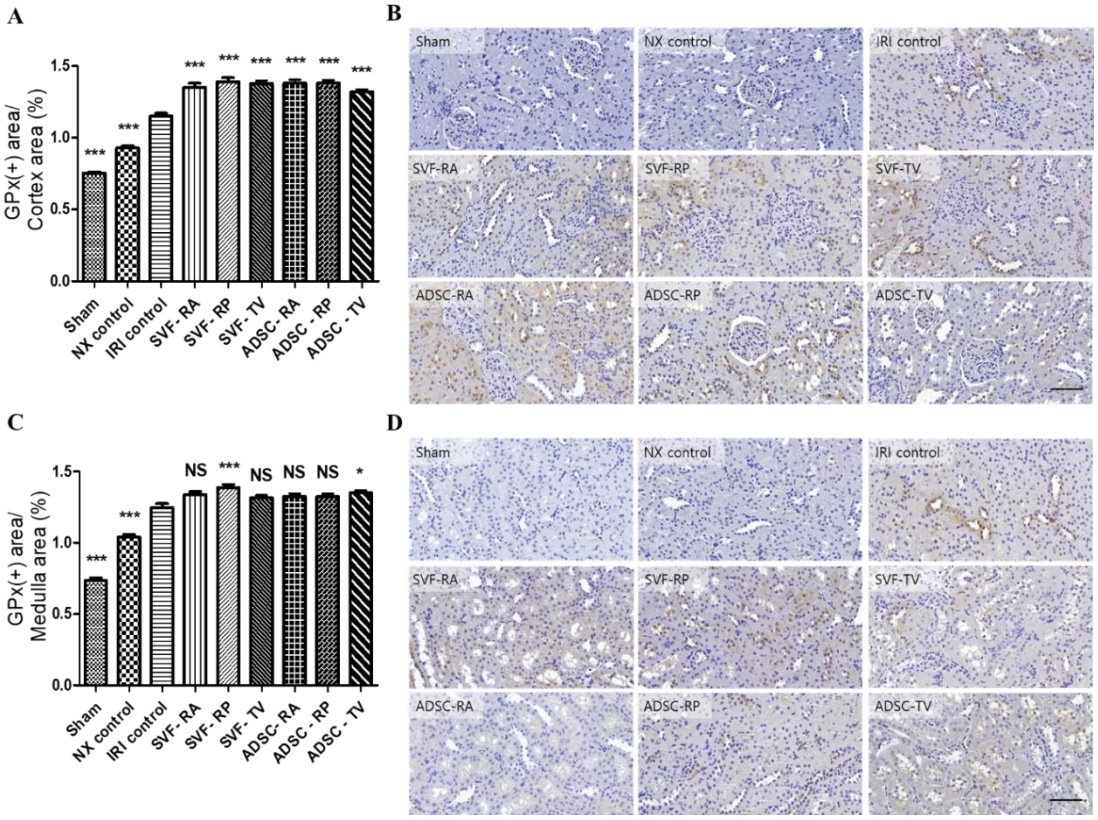

Figure10. GPx stain for determining the degree of Anti-oxidation. (A) Ratio of the area stained positive for GPx to the random cortex area and (B) representative photomicrographs. (C) Ratio of the area stained positive for GPx to the random medulla area and (D) representative photomicrographs. Scale bar 100 μm. NS, $P > 0.05$; *, $P < 0.05$; ***, $P < 0.001$ compared with the IRI control group.

Abbreviations: ADSC, adipose-derived stem cell; IRI, ischemia-reperfusion injury; NX, nephrectomy; RA, renal arterial; RP, renal parenchymal; SVF, stromal vascular fraction; TV, tail venous.

SVF and ADSC Localization with PKH-26

Two weeks after injection in all the treated groups, neither PKH-26-labeled SVF nor ADSC were found in the kidney (Figure 11).

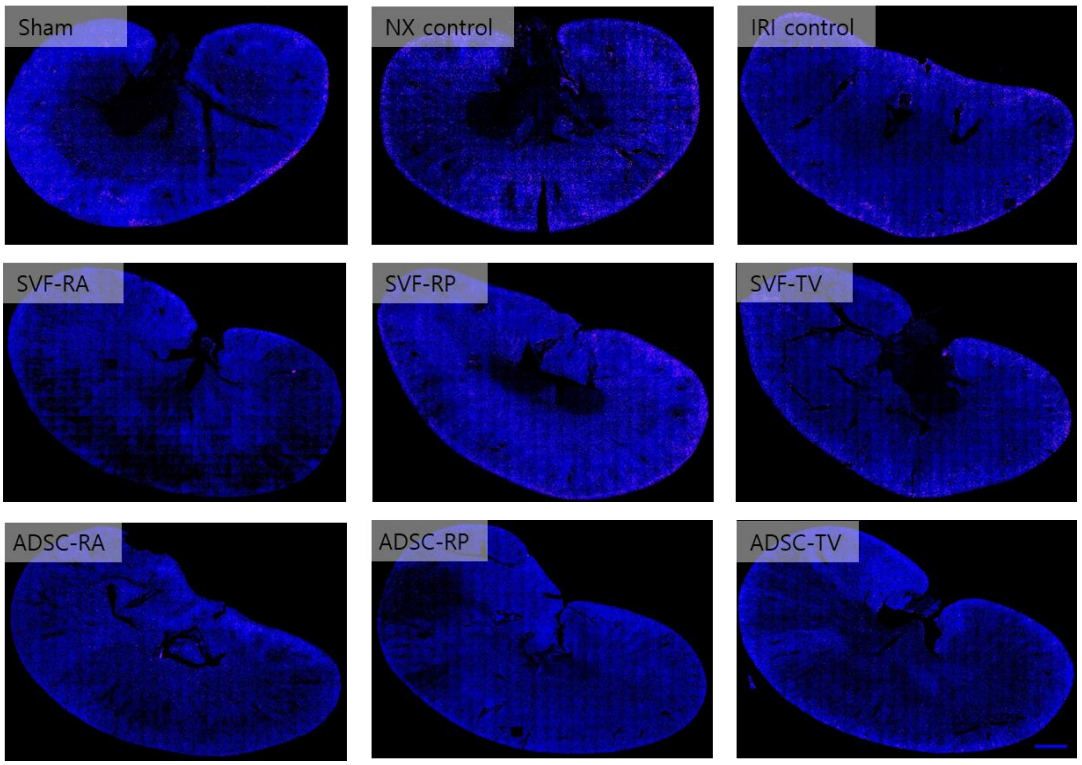

Figure11. Determination of PKH-26-labeled SVF and ADSC.

PKH-26-labeled SVF and ADSC were observeed by fluorescent microscope. Scale bar 2000 μm. Abbreviations: ADSC, adipose-derived stem cell; IRI, ischemia-reperfusion injury; NX, nephrectomy; RA, renal arterial; RP, renal parenchymal; SVF, stromal vascular fraction; TV, tail venous.

DISCUSSION

Many preclinical studies have investigated the effects of cultured and uncultured cells isolated from various sources to treat AKI including renal IRI [28, 29]. Adipose tissue is an attractive source of cultured and uncultured cells for tissue repair and regeneration for several reasons. First, humans have abundant subcutaneous fat deposits, which can be easily harvested using liposuction procesures[25, 30]. Second, ADSC have similar characteristics to bone marrow-derived MSC [31, 32]. Third, the proportions of MSC in bone marrow are between 1 in 25,000 to 1 in 100,000 cells, whereas ADSC constitute approximately 2% of lipoaspirated cells [33].

However, ADSC have some limitations, including the cost and time of culturing, the potential risk of contamination, changes in cell characteristics during culturing procedures, and tumorigenesis [17]. Because of these limitations, preclinical studies using SVF are increasing in renal diseases [9-13]. It was suggested that various angiogenic factors secreted by SVF, such as hepatocyte growth factor (HGF), vascular endothelial growth factor-A, and stromal cell-derivated factor-1α play important roles in the recovery of renal function [22]. There is little clinical trial to underway to examine the efficacy and safety of the use of SVF treating renal IRI. The optimal route for efficient and safe cell delivery is also little known in renal IRI [14]. Depending on route of delivery, cells may localize in the target organ or become trapped in non-target organs including lung causing adverse effects and diminish therapeutic efficacy [34, 35]. This led us to perform this study, which investigated the differences of SVF or ADSC, injected via three different routes, on renal IRI in terms of effectiveness and possible mechanisms of action.

We found that renal parenchymal injection of SVF restored most effectively renal function in a rat model of renal IRI. Moreover, only renal parenchymal SVF injection group was significantly superior to the IRI control group in terms of all histomorphometric studies

except histopathological scoring. Additionally, significant increase in GFR at 4 days after IRI as detected in the tail venous SVF injection group. However, studies investigating renal IRI have shown contradictory results according to cell sources or delivery routes. Zhou *et al.* [22] compared renal parenchymal injection of xenogeneic SVF and ADSC *in vivo* and showed equal effectiveness in attenuating renal IRI. Unlike their study, our study demonstrated that only SVF showed significant attenuation of renal IRI. There are several explanations for this difference between two studies. First, Zhou *et al.* [22] even reported that SVF showed stronger enhancement of renal tubular cell proliferation to ADSC *in vitro* with the more secretion of HGF by SVF. HGF can enhance the proliferation activity of renal tubular cell. Another explanation is that they used xenogeneic SVF and ADSC whereas we used autologous SVF and ADSC. ADSC have no immune response [36, 37], but SVF consisting of heterogeneous cell populations including blood-derived cells, endothelial (progenitor) cells, pericytes, and adipose-derived stromal cells can cause an immune response for xenotransplantation. Therefore, xenogeneic SVF are less effective than autologous SVF. The ineffectiveness of ADSC in our study might, at least in part, be attributable to the less number of cells than their study (1×10^6 vs 2×10^6 cells).

In terms of delivery routes, Yasuda K et al. [10] reported that subcapsular injection of autologous SVF limits renal injury via promoting renal capillary regeneration and proliferating renal tubular cells. Our previous study evaluated optimal route for autologous SVF delivery and found modest effectiveness in subcapsular injection [15]. Cheng et al. [38] reported that subcapsular transplanted MSC survived over longer periods, but they did not enter renal parenchyme. It has been appeared that transplanted MSC provide protection against AKI via paracrine signaling rather than by replacement of the damaged cells. We also did not find PKH-26-labeled SVF or ADSC in the kidney two weeks after injection. This finding might support such a hypothesis. Obviously, renal arterial injection can deliver cells efficiently by avoiding filtering organs, thus it is expected to provide the kidney with the

highest cell concentration. Our previous study also showed significant effectiveness in renal arterial infusion of SVF [15]. However, our present study did not replicate this finding. In our present study, the renal arterial injection was performed via aortic puncture, not direct renal arterial puncture, which was used in our previous study. This might be one of possible explanations for differences between two our studies. Moreover, intra-coronary arterial injection of cultured cells has been reported to cause microvascular obstruction due to culture hypertrophy [39,40]. Tatsumi *et al.* [41] showed that a factor responsible for promoting ADSC-mediated blood clotting is tissue factor (TF) expression at the cell surface. Unlike ADSC, SVF showed little coagulant activity in an *in vitro* coagulation assay. TF was rarely detected on the cell surface of SVF by immunostaining, and TF mRNA expression in SVF was only a tenth of that in ADSC. For that reason, renal arterial injection of cultured cells can result in vascular obstruction. Therefore, renal parenchymal injection can achieve maximum effectiveness while using a limited number of cells and avoiding the possible adverse effects.

Our study has several limitations. First, the exact composition of rat SVF was not examined. Second, rats were followed for only 2 weeks. The more long-term study not only evaluate the effects of cell-based therapies on AKI following renal IRI, but also whether it can prevent progression to chronic kidney disease. Zhou *et al.* [42] reported that preischemic administration of SVF reduced serum creatinine level at six months after renal IRI and inhibited renal fibrosis and then reduced the progression of chronic kidney disease. Third, rats were injected only once with a fixed dose (1×10^6) and concurrently with renal IRI. If repeat injections are shown to have synergistic effect, ADSC would be better because they can be kept in a freezer without a marked loss of cell viability and can be expanded easily without additional liposuction. Lastly, the baselines GFR were different among the groups, making it a problem for accurate results analysis. In subsequent experiments, GFR analysis was performed on all subjects before surgery, and subjects were divided according to the

numerical value, and GFR equalized baselines among groups.

Nevertheless, the findings from our study suggest that renal parenchymal injection of autologous SVF holds promise as a simple therapeutic approach for the treatment of predictable injury that might be induced by kidney surgery, such as kidney transplantation from deceased donors, on-pump cardiac surgery and nephron-sparing surgery .

CONCLUSIONS

Our study suggests that renal function is effectively rescued from renal IRI through renal parenchymal injection of SVF by enhanced anti-fibrotic, anti-apoptotic and anti-oxidative effects. The SVF therapy experimented in our study reveals important clues for future research, including large animal experiments or clinical studies.

ACKNOWLEDGEMENTS

This research was supported by National Research Foundation of Korea (NRF) grant funded by the Ministry of Science and ICT (MSIT), Republic of Kore (Grant No. 2015R1C1A1A01054399).

REFERENCES

1. Thadhani R, Pascual M, Bonventre JV. Acute renal failure. *N Engl J Med* 1996;334:1448-1460
2. Schrier RW, Wang W, Poole B, Mitra A. Acute renal failure:definitions, diagnosis, pathogenesis, and therapy. *J Clin Invest* 2004;114:5-14
3. Wang Y, He J, Pei X, Zhao W. Systematic review and meta-analysis of mesenchymal stem/stromal cells therapy for impaired renal function in small animal models. *Nephrology (Carlton)* 2013;18:201-208
4. Li B, Cohen A, Hudson TE, Motlagh D, Amrani DL, Duffield JS. Mobilized human hematopoietic stem/progenitor cells promote kidney repair after ischemia/reperfusion injury. *Circulation* 2010;121:2211-2220.
5. Tögel F, Weiss K, Yang Y, Hu Z, Zhang P, Westenfelder C. Vasculotropic, paracrine actions of infused mesenchymal stem cells are important to the recovery from acute kidney injury. *Am J Physiol Renal Physiol* 2007;292:F1626-F1635
6. Bi B, Schmitt R, Israilova M, Nishio H, Cantley LG. Stromal cells protect against acute tubular injury via an endocrine effect. *J Am Soc Nephrol* 2007;18:2486-2496
7. Dekel B, Shezen E, Even-Tov-Friedman S, Katchman H, Margalit R, Nagler A, Reisner Y. Transplantation of human hematopoietic stem cells into ischemic and growing kidneys suggests a role in vasculogenesis but not tubulogenesis. *Stem Cells* 2006;24:1185-1193
8. Tögel F, Westenfelder C. Mesenchymal stem cells: a new therapeutic tool for AKI. *Nat Rev Nephrol* 2010;6:179-183.
9. Feng Z, Ting J, Alfonso Z, Strem BM, Fraser JK, Rutenberg J, Kuo HC, Pinkernell K. Fresh and cryopreserved, uncultured adipose tissue-derived stem and regenerative cells

ameliorate ischemia-reperfusion-induced acute kidney injury. *Nephrol Dial Transplant* 2010 Dec; 25: 3874–3884.

10. Yasuda K, Ozaki T, Saka Y,Yamamoto T, Gotoh M, Ito Y, Yuzawa Y, Matsuo S, Maruyama S. Autologous cell therapy for cisplatin-induced acute kidney injury by using non-expanded adipose tissue-derived cells. *Cytotherapy* 2012;14: 1089–1100.
11. Li K, Han Q, Yan X, Liao L, Zhao R. C. Not a process of simple vicariousness, the differentiation of human adipose-derived mesenchymal stem cells to renal tubular epithelial cells plays an important role in acute kidney injury repairing. *Stem Cells Dev* 2010;19:1267-1275.
12. Chen YT, Sun CK, Lin YC, Chang LT, Chen YL, Tsai T H, Chung SY, Chua S, Kao YH, Yen CH, Shao PL, Chang KC, Leu S, Yip HK. Adipose-derived mesenchymal stem cell protects kidneys against ischemia-reperfusion injury through suppressing oxidative stress and inflammatory reaction. *J Transl Med* 2011;9:51
13. Shih YC, Lee PY, Cheng H, Tsai CH, Ma H, Tarng DC. Adipose-derived stem cells exhibit antioxidative and antiapoptotic properties to rescue ischemic acute kidney injury in rats. *Plast Reconstr Surg* 2013;132:940e-51e.
14. Jang MJ, You D, Park JY, Kim K, Aum J, Lee C, Song G, Shin HC, Suh N, Kim YM, Kim CS. Hypoxic Preconditioned Mesenchymal Stromal Cell Therapy in a Rat Model of Renal Ischemia-reperfusion Injury: Development of Optimal Protocol to Potentiate Therapeutic Efficacy. *Int. J. Stem Cells* 2018;11,157–167.
15. Lee C, Jang MJ, Kim BH, Park JY, You D, Jeong IG, Hong JH, Kim CS. Recovery of renal function after administration of adipose-tissue-derived stromal vascular fraction in rat model of acute kidney injury induced by ischemia/reperfusion injury. *Cell Tissue Res* 2017;368:603-613

16. Zhao L, Hu C, Zhang P, Jiang H, Chen J. Preconditioning strategies for improving the survival rate and paracrine ability of mesenchymal stem cells in acute kidney injury. *J Cell Mol Med* 2019;23:720–730.
17. Ning H, Liu G, Lin G, Garcia M, Li LC, Lue TF, Lin CS. Identification of an aberrant cell line among human adipose tissue-derived stem cell isolates. *Differentiation* 2009;77:172–180.
18. Granel B, Daumas A, Jouve E, Harlé JR, Nguyen PS, Chabannon C, Colavolpe N, Reynier JC, Truillet R, Mallet S, Baiada A, Casanova D, Giraudo L, Arnaud L, Veran J, Sabatier F, Magalon G. Safety, tolerability and potential efficacy of injection of autologous adipose-derived stromal vascular fraction in the fingers of patients with systemic sclerosis: An open-label phase I trial. *Ann Rheum Dis* 2015;74:2175–2182.
19. SVF (Adipose Tissue Derived MSC) Based Therapy for CKD. (StemCell&CKD). Available at https://clinicaltrials.gov/ct2/show/NCT03939741. Accessed April 09, 2020.
20. Effect of SVF Derived MSC in DCD Renal Transplantation. Available at https://clinicaltrials.gov/ct2/show/NCT02492490. Accessed April 09, 2020.
21. Induction With SVF Derived MSC in Living-related Kidney Transplantation. Available athttps://clinicaltrials.gov/ct2/show/NCT02492308. Accessed April 09, 2020.
22. Zhou L, Song Q, Shen J, Xu L, Xu Z, Wu R, Ge Y, Zhu J, Wu J, Dou Q, Jia R.Comparison of human adipose stromal vascular fraction and adiposederived mesenchymal stem cells for the attenuation of acute renal ischemia/ reperfusion injury. *Sci Rep* 2017;7:44058.
23. Zuk PA, Zhu M, Mizuno H, Huang J, Futrell JW, Katz AJ, Benhaim P, Lorenz HP, Hedrick MH. Multilineage cells from human adipose tissue: Implications for cell-based therapies. *Tissue Eng* 2001;7:211–228.

24. Zuk PA, Zhu M, Ashjian P, De Ugarte DA, Huang JI, Mizuno H, Alfonso ZC, Fraser JK, Benhaim P, Hedrick MH. Human adipose tissue is a source of multipotent stem cells. *Mol Biol Cell* 2002;13:4279–4295.

25. Bourin P, Bunnell BA, Casteilla L, Dominici M, Katz AJ, March KL, Redl H, Rubin JP, Yoshimura K, Gimble JM. Stromal cells from the adipose tissue-derived stromal vascular fraction and culture expanded adipose tissue-derived stromal/stem cells: A joint statement of the International Federation for Adipose Therapeutics and Science (IFATS) and the International Society for Cellular Therapy (ISCT). *Cytotherapy* 2013;15:641–648.

26. You D, Jang MJ, Kim BH, Song G, Lee C, Suh N, Jeong IG, Ahn TY, Kim CS Comparative study of autologous stromal vascular fraction and adipose-derived stem cells for erectile function recovery in a rat model of cavernous nerve injury. *Stem Cells Transl Med* 2015;4:351–358

27. Melnikov VY, Faubel S, Siegmund B, Lucia MS, Ljubanovic D, Edelstein CL. Neutrophil-independent mechanisms of caspase-1- and IL-18-mediated ischemic acute tubular necrosis in mice. *J Clin Invest* 2002;110:1083-1091.

28. Marcheque J, Bussolati B, Csete M, Perin L. Concise Reviews: Stem Cells and Kidney Regeneration: An Update. *Stem Cells Transl Med* 2019;8:82-92.

29. Rota C, Morigi M, Imberti B. Stem Cell Therapies in Kidney Diseases: Progress and Challenges. *Int J Mol Sci* 2019;20:2790.

30. Wilson A, Butler PE, Seifalian AM. Adipose-derived stem cells for clinical applications: A review. *Cell Prolif* 2011;44:86–98.

31. Lin G, Banie L, Ning H, Bella AJ, Lin CS, Lue TF. Potential of adipose-derived stem cells for treatment of erectile dysfunction. *J Sex Med* 2009;6(suppl 3):320–327.

32. Ning H, Liu G, Lin G Yang R, Lue TF, Lin CS. Fibroblastgrowth factor 2 promotes endothelial differentiation of adipose tissue-derived stem cells. *J Sex Med* 2009;6:967–979.

33. Barrilleaux B, Phinney DG, Prockop DJ, O'Connor KC. Review: Ex vivo engineering of living tissues with adult stem cells. *Tissue Eng* 2006; 12:3007–3019.

34. Freyman T, Polin G, Osman H, Crary J, Lu M, Cheng L, Palasis M, Wilensky RL. A quantitative, randomized study evaluating three methods of mesenchymal stem cell delivery following myocardial infarction. *Eur Heart J* 2006;27:1114–1122.

35. Fischer UM, Harting MT, Jimenez F, Monzon-Posadas WO, Xue H, Savitz SI, Laine GA, Cox CS Jr. Pulmonary passage is a major obstacle for intravenous stem cell delivery: The pulmonary firstpass effect. *Stem Cells Dev* 2009;18:683–692.

36. Puissant B, Barreau C, Bourin P, Clavel C, Corre J, Bousquet C, Taureau C, Cousin B, Abbal M, Laharrague P, Penicaud L, Casteilla L, Blancher A. Immunomodulatory effect of human adipose tissue-derived adult stem cells: comparison with bone marrow mesenchymal stem cells. *Br J Haematol* 2005;129:118-129.

37. McIntosh K, Zvonic S, Garrett S, Mitchell JB, Floyd ZE, Hammill L, Kloster A, Di Halvorsen Y, Ting JP, Storms RW, Goh B, Kilroy G, Wu X, Gimble JM. The immunogenicity of human adipose-derived cells: temporal changes in vitro. *Stem Cells* 2006;24:1246-1253.

38. Cheng K, Rai P, Plagov A, Lan X, Kumar D, Salhan D, Rehman S, Malhotra A, Bhargava K, Palestro CJ, Gupta S, Singhal PC. Transplantation of bone marrow-derived MSCs improves cisplatinum-induced renal injury through paracrine mechanisms. *Experimental and molecular pathology* 2013;94:466–473.

39. Vulliet PR, Greeley M, Halloran SM, MacDonald KA, Kittleson MD. Intra-coronary arterial injection of mesenchymal stromal cells and microinfarction in dogs. *Lancet* 2004;363:783–784.

40. Moelker AD, Baks T, Wever KM, Spitskovsky D, Wielopolski PA, van Beusekom HM, van Geuns RJ, Wnendt S, Duncker DJ, van der Giessen WJ. Intracoronary delivery of umbilical cord blood derived unrestricted somatic stem cells is not suitable to improve LV function after myocardial infarction in swine. *J Mol Cell Cardiol* 2007;42:735–745.
41. Tatsumi K, Ohashi K, Matsubara Y, Kohori A, Ohno T, Kakidachi H, Horii A, Kanegae K, Utoh R, Iwata T, Okano T. Tissue factor triggers procoagulation in transplanted mesenchymal stem cells leading to thromboembolism. *Biochem Biophys Res Commun* 2013;431:203-209.
42. Zhou L, Xu L, Shen J, Song Q, Wu R, Ge Y, Xin H, Zhu J, Wu J, Jia R. Preischemic Administration of Nonexpanded Adipose Stromal Vascular Fraction Attenuates Acute Renal Ischemia/Reperfusion Injury and Fibrosis. *Stem Cells Transl Med* 2016;5:1277-1288.

KOREAN ABSTRACTS

신장의 허혈-재관류 손상 랫트 모델에서 신기능 회복을 위한 자가 기질혈관분획 및 지방유래 줄기세포의 비교 연구

신장의 허혈-재관류 손상에서 상이한 지방유래 세포치료제를 비교하거나, 효율적이고 안전한 세포 전달을 위한 최적의 경로를 비교한 연구는 거의 없다. 본 연구에서는 신장의 허혈-재관류 손상 랫트 모델에서 세가지 상이한 경로를 통해 주입된 자가 기질혈관분획과 지방유래 줄기세포의 신기능 보호 능력을 비교하였다. 90 마리의 Sprague-Dawley 랫트를 무작위로 9 개의 그룹으로 분류하였다: 거짓 수술군, 신절제 대조군, 허혈-재관류 손상 대조군, 기질혈관분획 신동맥 주입군, 기질혈관분획 신실질 주입군, 기질혈관분획 꼬리정맥 주입군, 지방유래 줄기세포 신동맥 주입군, 지방유래 줄기세포 신실질 주입군, 지방유래 줄기세포 꼬리정맥 주입군. 신기능은 허혈-재관류 손상을 유도하기 위한 수술 4 일 전 및 1, 2, 3, 4, 7, 14 일 후에 평가하였다. 조직형태학적 연구는 수술 14 일 후에 수행하였다. 기질혈관분획 신실질 주입은 허혈-재관류 손상 대조군과 비교하여 혈청 혈액요소질소 및 크레아티닌의 상승 정도를 유의하게 줄였다. 기질혈관분획 신실질 주입은 허혈-재관류 손상 대조군에 비해 사구체여과율의 감소 정도를 유의하게 줄였다. 또한, 콜라겐 함량은 허혈-재관류 손상 대조군보다 기질혈관분획 신실질 주입군에서 더 낮았다. 기질혈관분획 신실질 주입은 허혈-재관류 손상 대조군과 비교하여 세포자멸은 감소시켰으며, 세포증식은 증가시켰다. 글루타티온 환원효소 및 글루타티온 퍼옥시다제와 같은 항산화 표지자의 발현은 허혈-재관류 손상

대조군보다 기질혈관분획 신실질 주입군에서 더 높았다. 본 연구는 기질혈관분획 신실질 주입이 강화된 항섬유화, 항세포자멸 및 항산화 효과에 의해 신장의 허혈-재관류 손상으로부터 신기능을 효과적으로 구제함을 시사한다.